Cell surface Notch ligand DLL3 is a therapeutic target in isocitrate dehydrogenase mutant glioma

Marissa Spino[1,*], **Sylvia C. Kurz**[2,*], **Luis Chiriboga**[#1,*], **Jonathan Serrano**[1], **Briana Zeck**[1], **Namita Sen**[2], **Seema Patel**[1], **Guomiao Shen**[1], **Varshini Vasudevaraja**[1], **Carter M. Suryadevara**[3], **Joshua Frenster**[3], **Kensuke Tateishi**[4], **Hiroaki Wakimoto**[5], **Rajan Jain**[2,6], **Howard A. Riina**[3], **Theodore P. Nicolaides**[2,7], **Erik P. Sulman**[2,8,9], **Daniel P. Cahill**[5], **John G. Golfinos**[2,3], **Kumiko Isse**[10], **Laura R. Saunders**[10], **David Zagzag**[1,2], **Dimitris Placantonakis**[2,3], **Matija Snuderl**[1,2,#], **Andrew S. Chi**[2,#]

[1]Department of Pathology, NYU Langone Health, New York, NY, USA

[2]Laura and Isaac Perlmutter Cancer Center, NYU Langone Health, New York, NY, USA

[3]Department of Neurosurgery, NYU Langone Health, New York, NY, USA

[4]Department of Neurosurgery, Yokohama City University School of Medicine, Yokohama, Japan

[5]Department of Neurosurgery, Massachusetts General Hospital, Boston, MA, USA

[6]Department of Radiology, NYU Langone Health, New York, NY, USA

[7]Department of Pediatrics, NYU Langone Health, New York, NY, USA

[8]Departments of Radiation Oncology, Translational Molecular Pathology, and Genomic Medicine, The University of Texas MD Anderson Cancer Center, Houston, TX, USA

[9]Department of Radiation Oncology, NYU Langone Health, New York, NY, USA

[10]AbbVie Stemcentrx LLC

[#] These authors contributed equally to this work.

Abstract

Purpose: Isocitrate dehydrogenase (*IDH*) mutant gliomas are a distinct glioma molecular subtype for which no effective molecularly-directed therapy exists. Low-grade gliomas, which are 80–90% *IDH* mutant, have high RNA levels of the cell surface Notch ligand DLL3. We sought to determine DLL3 expression by immunohistochemistry in glioma molecular subtypes and the potential efficacy of an anti-DLL3 antibody drug conjugate (ADC), rovalpituzumab tesirine (Rova-T), in *IDH* mutant glioma.

Corresponding Author: Andrew S. Chi, MD, PhD, 240 E. 38th Street, 19th Floor, New York, NY 10011, Tel: 212-731-6267, Fax: 646-754-9696, chia01@nyumc.org.
*Equal contributions
#Co-senior author

Experimental Design: We evaluated *DLL3* expression by RNA using TCGA data and by immunohistochemistry in a discovery set of 63 gliomas and 20 non-tumor brain tissues and a validation set of 62 known *IDH* wildtype and mutant gliomas using a monoclonal anti-DLL3 antibody. Genotype was determined using a DNA methylation array classifier or by sequencing. The effect of Rova-T on patient-derived endogenous *IDH* mutant glioma tumorspheres was determined by cell viability assay.

Results: Compared to *IDH* wildtype glioblastoma, *IDH* mutant gliomas have significantly higher DLL3 RNA ($P<1\times10^{-15}$) and protein by immunohistochemistry ($P=0.0014$ and $P<4.3\times10^{-6}$ in the discovery and validation set, respectively). DLL3 immunostaining was intense and homogeneous in *IDH* mutant gliomas, retained in all recurrent tumors, and detected in only 1 of 20 non-tumor brains. Patient-derived *IDH* mutant glioma tumorspheres overexpressed DLL3 and were potently sensitive to Rova-T.

Conclusions: DLL3 is selectively and homogeneously expressed in *IDH* mutant gliomas and can be targeted with Rova-T in patient-derived *IDH* mutant glioma tumorspheres. Our findings have potential for rapid clinical translation and may impact therapeutic strategies that exploit cell surface tumor-specific antigens.

Keywords

Introduction

Mutations in the isocitrate dehydrogenase (*IDH*) 1 and *IDH2* genes identify a subtype of glioma with distinct biological, clinical and radiographic features (1–5). These gliomas develop through early mutation of *IDH* (6), which results in accumulation of 2-hydroxyglutarate (7) and a genome-wide DNA hypermethylation phenotype (8), followed by acquisition of one of two sets of co-occurring genetic alterations: *TP53* and *ATRX* mutations, or 1p/19q codeletion and mutations in *TERT*, *CIC* and *FUBP1* (9–12). More recent studies have identified a small subset of more aggressive *IDH* mutant gliomas associated with lower global DNA methylation (13) and homozygous *CDKN2A/B* deletion (14), and alterations that are frequently acquired at recurrence, including temozolomide-induced hypermutation phenotype (15), Myc pathway alterations (16), and driver oncogenes and tumor suppressors (15–17).

The recent success in identifying the genetic alterations driving the development and progression of *IDH* mutant glioma has yet to translate into successful novel therapies, however. Standard adjuvant treatment consisting of radiation and the procarbazine, CCNU, vincristine (PCV) chemotherapy regimen improves survival of *IDH* mutant glioma patients (18, 19); however, most tumors eventually recur and are lethal. Due to the challenges experienced in directly targeting alterations driving *IDH* mutant gliomagenesis, recent efforts have focused on immunotherapy and synthetic lethal strategies to selectively target *IDH* mutant gliomas (20–23). However, these approaches await clinical validation.

The cell surface Notch ligand delta-like 3 (DLL3) has recently emerged as a therapeutic target in cancer, pioneered in pulmonary neuroendocrine tumors (24). A critical mediator of cellular development, DLL3 inhibits Notch pathway activation in cis and in trans by redirecting or retaining Notch and the Notch activating ligand DLL1 to late endosomal/ lysosomal compartments or the Golgi, respectively, and preventing their localization to the cell surface (25, 26). While DLL3 is predominantly localized to the Golgi apparatus (25, 27), Saunders et al. recently confirmed diffuse DLL3 expression on the cell surface membrane of pulmonary neuroendocrine tumor cells (24). Together with the absence of DLL3 expression in normal lung tissue, this study established DLL3 as a tumor-associated antigen and a tractable therapeutic target, leading to the development of rovalpituzumab tesirine (Rova-T), a DLL3-targeting antibody-drug conjugate that is currently in clinical trials (24, 28).

In their investigation of DLL3, Saunders et al. found DLL3 expression by RNA-Seq to be the highest in low-grade gliomas among more than 20 cancer types in The Cancer Genome Atlas (TCGA) dataset (24). Because 80–90% of low-grade gliomas are *IDH* mutant (2, 3), we therefore hypothesized that DLL3 would be highly overexpressed in *IDH* mutant glioma and that expression would be tightly associated with *IDH* mutant gliomas compared to *IDH* wildtype glioma. Here, we analyzed a cohort of diffuse gliomas using immunohistochemistry (IHC) with an anti-DLL3 monoclonal antibody and compared DLL3 expression between glioma molecular subtypes. We then tested the therapeutic potential of the anti-DLL3 ADC Rova-T using patient-derived glioma tumorsphere cultures.

Materials and Methods

Tumor samples

For the discovery set, 20 non-tumor brain tissue samples and 63 glioma tumor samples were obtained from Cooperative Human Tumor Network (CHTN), Conversant Bio, and RS Diagnostics. This set of tumors included the following diagnoses: glioblastoma, WHO grade IV (n=30 including 1 recurrent tumor), oligodendroglioma, grade II (n=11), anaplastic oligodendroglioma, grade III (n=4, including 1 recurrent), 3 astrocytoma, grade II (n=3, including 1 recurrent), anaplastic astrocytoma, grade III (n=4, including 1 recurrent), "oligoastrocytoma", grade III (n=5), and one each of pilocytic astrocytoma, pleomorphic xanthoastrocytoma grade II, ependymoma grade II, mixed ependymoma-subependymoma, ganglioglioma and recurrent glioma NOS.

For the validation set, 62 gliomas with known *IDH1/2* mutation status were obtained from the NYU pathology database to compare DLL3 expression in *IDH* mutant glioma and *IDH* wildtype glioblastoma. This set included 26 *IDH* wildtype glioblastomas, including 1 recurrent tumor, and 36 *IDH* mutant glioma tumors from 25 patients. Within *IDH* mutant gliomas, there were 14 recurrent tumors, 11 of which had paired original tumors from the same patient. The pathological diagnoses in this set included astrocytoma grade II (n=10), anaplastic astrocytomas (n=3), oligodendroglioma, grade II (n=6), and anaplastic oligodendrogliomas, grade III (n=2). All tumor samples, pathological information, and molecular data were collected under NYU institutional review board approved protocols.

TCGA DLL3 mutation, copy number, and gene expression analyses

Glioma tumor mutation, copy number, and normalized mRNA (RNA-Seq V2) TCGA datasets were downloaded from www.cbioportal.org (29, 30). For DLL3 expression analysis, tumors from the Glioblastoma TCGA, Cell 2013 database (31) and Brain Lower Grade Glioma (TCGA, Provisional) database (32) with both *IDH1/2* mutation status and DLL3 RNA-Seq data available (a total of 433 tumors) were accessed on April 1, 2018. For DLL3 mutation and copy number analyses, all diffuse glioma, lower grade glioma (LGG), glioblastoma, medulloblastoma, and pilocytic astrocytoma datasets (total 4634 sequenced cases) were accessed on June 23, 2018.

DLL3 immunohistochemistry

For the discovery set, DLL3 immunohistochemistry (IHC) was performed on 5-mm-thick formalin-fixed, paraffin-embedded (FFPE) tissue sections using a proprietary monoclonal unconjugated, mouse anti-human DLL3, clone SC16.65 (Abbvie-Stemcentrx) optimized on 5-micron sections of human DLL3 over-expressing HEK-293T (HEK-293T.hDLL3, positive control) and naive HEK-293T cell lines (negative control) sectioned onto plus slides (Fisher Scientific, Cat # 22–042-924), or murine IgG2a isotype control on the Ventana platform (Ventana Medical Systems) as previously described (28). For the validation set, chromogenic IHC was performed using SC16.65 (provided by Abbvie-Stemcentrx), optimized on the same positive and negative control slides (HEK-293T.hDLL3 and naive HEK-293T cell lines) on the Ventana platform (Discovery XT instrument). Sections were incubated for 1 hour at 60°C. Sections were deparaffinized and antigen retrieved using Low pH, Envision Flex Retrieval solution in a Dako PT Link with preheat temperature of 65°C, retrieval temperature of 97°C for 20 minutes and cool-down end temperature of 65°C. Slides were rinsed with instrument reaction buffer and endogenous peroxidase activity was blocked. SC16.65 was diluted 1:4000 in Ventana diluent (Catalog# 251–018) and incubated for 1 hour at 37°C. Primary antibody was detected with goat anti-mouse horseradish peroxidase conjugated multimer incubated for 16 minutes. The complex was visualized with 3,3 diaminobenzidene and enhanced with copper sulfate. Slides were washed in distilled water, counterstained with hematoxylin, dehydrated and mounted with permanent media. Negative controls consisted of isotype (IgG2a, matched concentration) and primary antibody diluent substituted for primary antibody on sections of HEK-293T.hDLL3 cell line. A patient derived xenograft expressing endogenous DLL3 (24) and naive HEK-293T cell line were used as positive and negative controls and included with the study sections.

IHC scoring for the discovery set was performed independently by two teams; two board-certified neuropathologists (D.Z. and M.S) at NYU and a pathology researcher with more than 15 years of IHC experience at Abbvie Stemcentrx (K.I.). Scoring was performed blinded to the pathology report and diagnosis. At the time of scoring, the *IDH* mutation/molecular status of the tumor samples was undetermined. Surface DLL3 expression was quantified by counting the percentage of cells with expression and by converting the staining intensity (range, 0-no staining, 1-weak, 2-moderate, 3-strong) and the percentage of cells with expression to an H-score (range, 0 to 300). For the validation set, the DLL3 immunostained tumor samples were coded and randomized to blind the neuropathologists (M.S. and D.Z.), and surface DLL3 expression was scored following the same criteria.

Molecular analysis and determination of IDH mutation and 1p/19q codeletion status

In all tumors, DNA was extracted from FFPE. Areas with the highest available tumor content were chosen. Extraction was carried out using the automated Maxwell system (Promega, Madison, USA). DNA methylation was analyzed by the Illumina EPIC Human Methylation array assessing 850,000 CpG sites (MethylationEPIC BeadChip 850k microarray, Illumina, San Diego, USA), according to the manufacturer's instructions at the NYU Molecular Pathology laboratory as described previously (33).

For tumors in the discovery set, the glioma molecular subtype was determined using a recently developed random forest classifier tool (34) which analyzes whole-genome DNA methylation data generated from Illumina MethylationEPIC 850k arrays and classifies tumors into one of 82 designated CNS tumor classes. This DNA methylation classifier tool predicts *IDH*-mutant gliomas with high specificity and sensitivity, and also determines 1p/19q deletion status based on analysis of the copy number profile generated from 850k/EPIC data. Specifically, the methylation class family "Glioma, *IDH* mutant" comprises the methylation classes "astrocytoma, *IDH* mutant", "astrocytoma, IDH mutant, subtype high grade" and "oligodendroglioma, *IDH* mutant and 1p/19q codeleted". The methylation class family "Glioblastoma, *IDH* wildtype" comprises the subclasses RTK I to III, mesenchymal, *MYCN* and midline. Furthermore, this DNA methylation classifier tool determines *MGMT* promoter methylation status using the MGMT-STP27 model (35).

For tumors in the validation set, we included a set of known glioblastomas confirmed to be *IDH1/2* wildtype either by the DNA methylation classifier tool ("Glioblastoma, *IDH* wildtype") or by a clinical targeted next-generation sequencing (NGS) Ion Torrent hotspot panel that included all mutation hotspots of *IDH1* and *IDH2* (ThermoFisher Scientific, CA) with a minimal 500x coverage of target areas. All FFPE slides were reviewed and the slide/block with the highest tumor cell content, at minimum 80%, was utilized for molecular studies. For the *IDH* mutant glioma cohort in the validation set, *IDH* mutation status was determined by immunohistochemistry for IDH1 R132H or by the clinical targeted NGS panel. Four μm sections were cut from FFPE blocks from tumor specimens and stained with hematoxylin/eosin and examined by IHC with an antibody against IDH1 R132H (clone H09, Dianova).

1p/19q codeletion status for *IDH* mutant gliomas in the validation set was previously determined utilizing a loss of heterozygosity (LOH) PCR CLIA laboratory developed assay. Normal (peripheral blood mononuclear cell) and tumor DNA were extracted. The polymorphic chromosomal markers of 1p (7 loci, D1S1612, D1S430, D1S199, D1S224, DIS162, DIS171 and D1S1161) and 19q (4 loci, D19S601, D19S412, D19S112 and D19S559) were used to evaluate 1p/19q LOH in the tumor by PCR. The amplified PCR products were fluorescently labeled and were analyzed by capillary gel electrophoresis. Normal and tumor DNA were compared in order to determine whether there was allelic loss of chromosome 1p and/or 19q. To detect 1p/19q LOH, tumor tissue was no less than 75% of the total sample tissue.

Western blot

Western blots were performed as previously described (21) with modification to visualize using a LI-COR Odyssey Detection System (LI-COR Biosciences); membranes were blocked using LI-COR blocking buffer and IRDye (LI-COR) secondary antibodies were used. Primary antibodies used were: SP347 (anti-DLL3, provided by Abbvie Stemcentrx), anti-IDH1 R132H (clone H09, Dianova), GAPDH (ThermoFisher). Extracts of SHP77 (high DLL3 expression), NCI-H69 (low to moderate DLL3 expression) and NCI-H211 (no DLL3 expression) cells were provided by Abbvie Stemcentrx.

Cell culture

U87 cells constitutively expressing GFP (U87-GFP) or IDH1 R132H (U87-IDH) were engineered previously in our lab (21). U87-GFP, U87-IDH and HEK-293T cells were cultured in DMEM + 10% fetal bovine serum. The patient-derived glioma tumorspheres MGG18 (*IDH* wildtype), MGG119 (*IDH1* R132H mutant), MGG152 (*IDH1* R132H mutant) and MGG18-IDH, an *IDH* wildtype GBM line engineered with a doxycycline-inducible IDH1 R132H gene, were all previously derived in our laboratory and were cultured in serum-free neural stem cell medium as described (17, 21). To induce mutant *IDH1* expression, MGG18-IDH1 cells were cultured with doxycycline (Sigma-Aldrich, 1 μg/ml) for 72 hours.

Cell viability assay

Compounds used for cell viability assays included two antibody drug conjugates (ADCs): SC16LD6.5 (rovalpituzumab tesirine, Rova-T), which consists of SC16, an anti-DLL3 humanized monoclonal antibody, conjugated to LD6.5, a DNA-damaging pyrrolobenzodiazepine dimer toxin and IgGLD6.5, which consists of a non-targeting human IgG conjugated to LD6.5 (24). SC16LD6.5 and IgGLD6.5 were provided by Abbvie Stemcentrix.

Cells (500 for U87-GFP, U87-IDH, and HEK-293T; 4000 for MGG152; 8000 for MGG119) were dissociated in to single cells and seeded into 96-well plates at 50 μL per well on day 1. On day 2, SC16LD6.5 or IgGLD6.5 were serially diluted in culture media and added to wells and cells were cultured for 8 days. Each sample concentration was tested in triplicate. Cell viability was measured by CellTiter-Glo assay (Promega) according to the manufacturer's instructions, using a Synergy HTX multimode plate reader (Biotech US). The luminescence values for each sample-treated well were normalized to untreated well values, and percent cell viability was plotted as a function of sample concentration. Data were analyzed with GraphPad Prism software using a four-parameter logistic nonlinear regression model.

Statistical considerations

Nonparametric tests were used to compare groups in data generated by RNA-Seq and immunohistochemistry. The Wilcoxon–Mann–Whitney U test was used to compare two groups and the Kruskal-Wallis test was used when comparing more than two groups, with followup multiple comparison testing using Dunn's method with false discovery rate control using the two-stage linear step-up procedure of Benjamini, Krieger and Yekutieli. All *P*

values were two-tailed. Statistical tests were performed in GraphPad Prism 7 (La Jolla, CA, USA).

Results

DLL3 is overexpressed in IDH mutant glioma by RNA-Seq

Using TCGA datasets from 21 different cancer types, Saunders et al. found that low-grade glioma (LGG) had the highest DLL3 mRNA by RNA-Seq, while glioblastoma also had high expression relative to other cancers (24). Based on these data, we hypothesized that *IDH* mutant gliomas would have significantly elevated DLL3 expression, and within gliomas, DLL3 expression would be mainly associated with *IDH* mutant gliomas versus *IDH* wildtype glioma. To test this, we analyzed tumors in the TCGA LGG and glioblastoma datasets that had both *IDH1/2* mutation status annotated and DLL3 RNA-seq data available (Supplementary Table S1).

We initially compared *DLL3* expression by glioma grade. There was a significant difference between lower grade (WHO grade II and III) glioma (n=284) and glioblastoma (WHO grade IV) (n=147), with lower-grade gliomas having 3.2-fold higher expression (median read count 3726 *vs.* 1180, $P = 2.7 \times 10^{-9}$) (Figure 1). There was also a significant difference in DLL3 expression when separating grade II and III tumors [median read counts of 4467, 2935 and 1180 for grade II (n=139), III (n=145) and IV (n=147), respectively, $P = 3.1 \times 10^{-10}$] and when each grade was compared to another (grade II *vs.* grade III, $P = 0.0037$, grade II *vs.* grade IV, $P = 4.2 \times 10^{-11}$, grade III *vs.* grade IV, $P = 0.0002$), with a 3.8-fold difference between grade II and IV.

Given that 70–90% of grade II and III gliomas are *IDH* mutant (2, 3), we compared the difference between *IDH* mutant (n=241) *vs. IDH* wildtype (n=192) glioma and found a striking difference in DLL3 expression, with *IDH* mutant glioma harboring 5.2-fold greater DLL3 expression (median read count 4733 *vs.* 916, $P < 1 \times 10^{-15}$) (Figure 1). DLL3 overexpression in gliomas was not a consequence of *DLL3* mutations or gene amplification, as these events were exceedingly rare. Among all glial and neuronal tumors in the TCGA dataset with available sequence data, including diffuse gliomas, pilocytic astrocytomas, and medulloblastomas, only 4 tumors had *DLL3* gene amplification (all glioblastomas), 3 *DLL3* missense mutations were detected (two diffuse gliomas, one medulloblastoma), and 1 *DLL3* fusion was detected in an oligodendroglioma (Supplementary Table S2).

DLL3 expression is intense and homogeneous in IDH mutant glioma by immunohistochemistry

To confirm DLL3 protein expression in gliomas and assess the relationship of protein expression in different subtypes of glioma, we performed IHC using a highly specific monoclonal antibody for DLL3 (SC16.65) on a discovery set of 63 gliomas and 20 non-tumor brain tissue samples. DLL3 staining was scored independently at two different teams (Abbvie Stemcentrx and NYU) and scoring was blinded to the *IDH* mutation status and molecular subtype of the tumors. Representative images of DLL3 IHC are shown in Figure 2.

In addition to scoring DLL3 staining, DNA was extracted from available tumor FFPE scrolls in the discovery set (n=56) and analyzed using a DNA methylation array classifier tool to classifies glioma molecular subtype (34). In total, 46 tumors could be classified using the classifier tool; 10 tumors had no match due to insufficient or poor-quality tumor DNA (Figure 3, Table 1, Supplementary Table S3). There were 17 classified as *IDH* wildtype glioblastoma, 19 as *IDH* mutant gliomas (including nine *IDH* mutant, 1p/19q codeleted and 10 *IDH* mutant, non-codeleted tumors), and 10 tumors of other major designated classes. These 10 "other" tumors consisted of pediatric and young adult glioma variants including pilocytic astrocytoma, subependymoma, ganglioglioma.

Based on the differences in gene expression, we compared the DLL3 IHC scores by H-score (scored at Abbvie Stemcentrx) and percent of positive tumor cells (scored independently at NYU) between *IDH* mutant glioma and *IDH* wildtype glioblastoma and found a marked difference in DLL3 expression (P=0.0014 for H-score, P=0.003 for percent of DLL3 positive tumor cells) (Table 1, Figure 3). Notably, the majority of *IDH* mutant gliomas had intense and homogeneous membranous DLL3 expression, whereas expression in *IDH* wildtype glioblastoma was largely absent, and when present was patchy or scattered (Figure 2). This distribution was reflected in the IHC scoring; the median H-scores and the median proportion of DLL3 positive tumor cells was 250 and 80%, respectively, for *IDH* mutant glioma, and 15 and 15%, respectively, for *IDH* wildtype glioblastoma. Of note, 19 of 20 non-tumor brain tissue samples were negative for DLL3 while scattered neurons were positive for DLL3 in one sample, (Supplementary Figure S1), and DLL3 expression was only observed in a few of the glioma variants (Table 1).

Among *IDH* wildtype glioblastomas, approximately half (8/17, 47%) had either no expression or only scattered cells expressing DLL3. When expressed, scattered and patchy staining was characteristic of this subtype, and only 4 (24%) tumors expressed DLL3 in 50% of tumor cells, with no tumor (0/17) 80% positive (Table 1). By contrast, the majority of *IDH* mutant gliomas (11/19, 58%) had 80% DLL3 positive tumor cells. This homogeneity of DLL3 positivity in *IDH* mutant glioma compares favorably with pulmonary neuroendocrine tumors, where the mean DLL3 H-scores range from 125–200 (24).

We then collected a validation set of known *IDH* wildtype glioblastomas and known *IDH* mutant gliomas archived at NYU to test the association of DLL3 expression by IHC and *IDH* mutant glioma. We collected a set and performed IHC using the same anti-DLL3 antibody (Supplementary Table S4). In the validation set, we confirmed that DLL3 expression in *IDH* mutant glioma was intense, homogeneous, and significantly higher than in *IDH* wildtype glioblastoma, with median H-scores of 130 *vs.* 10 (P=4.3 × 10^{-6}) for *IDH* mutant glioma and *IDH* wildtype glioblastoma, respectively, and median proportion of positive tumor cells of 60% *vs.* 5% (P=1.7 × 10^{-7}), respectively (Table 1).

Additionally, we evaluated the expression of recurrent *IDH* mutant gliomas to assess whether DLL3 expression was retained at progression. We evaluated 14 recurrent tumors, of which 11 had paired original tumors, and found intense, homogeneous DLL3 expression in most cases (Figures 2,3). Interestingly, DLL3 expression was higher in the recurrent cases, and for most paired cases the recurrent tumor had higher expression, although these

differences were not statistically significant. One tumor was recurrent after radiation therapy (V010R), however, and DLL3 expression was retained in the progressive tumor (Supplementary Table S4).

DLL3 expression in glioma molecular subtypes

Because both *IDH* mutant glioma and *IDH* wildtype glioblastoma can each be further subdivided into molecularly distinct subtypes, we explored whether DLL3 expression differed between these subtypes. In the discovery set, we found that high DLL3 expression was nearly universal in the 1p/19q codeleted subtype of *IDH* mutant glioma (Supplementary Tables S4, S5). All *IDH* mutant, 1p/19q codeleted gliomas expressed DLL3, with the lowest H-score being 50, while in 8 of 9 (89%) tumors DLL3 was positive in 50% of tumor cells and in 6 of 9 (67%) DLL3 was positive in at least 90% of tumor cells, including two high-grade (grade III) tumors. Among *IDH* mutant, non-codeleted gliomas (astrocytoma subclass), DLL3 expression was also high although not to the same extent. In the discovery set, there was a significant difference in DLL3 expression between the two subclasses (*P*=0.012 for H-score, *P*=0.01 for percent of positive tumor cells), with median H-scores and DLL3 positive tumor cell proportions of 270 and 90%, respectively, for the 1p/19q codeleted subclass and 85 and 55%, respectively, for the astrocytoma subclass. In the validation set, however, there was no statistically significant difference between the astrocytoma and 1p/19q codeleted subset of *IDH* mutant gliomas (Figure 4, Supplementary Table S6).

In the *IDH* mutant, astrocytoma subclass half (5 of 10) had at least 50% of tumor cells DLL3 positive, including 4 (40%) with 80% DLL3 positive tumor cells. A subset (4/10, 40%) of *IDH* mutant astrocytomas had little to no DLL3 expression, and 3 (75%) of these tumors were molecularly high-grade. However, there was no statistically significant difference in DLL3 expression between low-grade and high-grade astrocytomas in this subclass. Notably, there were two glioblastomas in the molecular *IDH* mutant astrocytoma set, with tumor cells positive in only 5% in one and 80% in the other. Similar to the discovery set, only 2 of 25 (8%) *IDH* mutant gliomas in the validation set lacked DLL3 expression, both were astrocytomas (Figure 4, Supplementary Tables S4, S5).

IDH wildtype glioblastoma can be subclassified into two robust prognostic and biological groups based on the status of *MGMT* promoter methylation (36, 37). Among *IDH* wildtype glioblastomas in the discovery set, all 4 tumors with DLL3 expression in 50% of tumor cells were *MGMT* methylated. There was a trend towards lower DLL3 expression in *MGMT* unmethylated tumors, although this difference did not reach statistical significance (median H-score 4.5 for *MGMT* unmethylated *vs.* 27.5 for *MGMT* methylated, *P*=0.11; and median DLL3 positive tumor cells 5% for *MGMT* unmethylated *vs.* 25% for *MGMT* methylated, *P*=0.12). In the validation set, there was no significant difference between *MGMT* methylated and *MGMT* unmethylated tumors in DLL3 expression; however, expression of all *IDH* wildtype glioblastoma was lower in the validation set compared to the discovery set (Figure 4, Supplementary Tables S4, S5).

In addition, the DNA methylation array classifier tool divides *IDH* wildtype glioblastoma into several phenotypic subclasses (34). The classifier tool subclasses identified in the discovery set of *IDH* wildtype glioblastoma included "RTKI" (n=3), "RTKII" (n=7), and

"Mesenchymal" (n=6). Because previous glioblastoma expression profiling subtyping studies have reported DLL3 overexpression in proneural tumors and no expression in Mesenchymal tumors (38, 39), we compared DLL3 expression in DNA methylation classifier-defined Mesenchymal tumors to other classifier subtypes. We found that DLL3 expression, if present in *IDH* wildtype glioblastoma, to be generally restricted to non-Mesenchymal tumors [median H-score 0 for Mesenchymal *vs.* 42.5 for non-Mesenchymal, *P*=0.019; median positive DLL3 tumor cells 5% for Mesenchymal *vs.* 35% for non-Mesenchymal, *P*=0.0037]. However, in the validation set, the H-score difference between Mesenchymal and non-Mesenchymal tumors only trended to significance (median 0.5 vs. 10, *P*=0.08) (Figure 4, Supplementary Tables S4, S5).

An anti-DLL3 antibody-drug conjugate is cytotoxic to DLL3-expressing patient-derived IDH mutant glioma tumorsphere cultures

We then assessed whether DLL3 represents a therapeutic target in *IDH* mutant glioma cells. We first confirmed by Western blot that our patient-derived, endogenous *IDH* mutant glioma tumorsphere lines MGG119 and MGG152 expressed DLL3 (17) (Figure 5). Interestingly, we did not find that introducing IDH1 R132H into glioma cells induced DLL3 expression. Malignant glioma cells engineered to constitutively overexpress IDH1 R132H (U87-*IDH*) and an *IDH* wildtype patient-derived glioblastoma tumorsphere line engineered with doxycycline-inducible *IDH1^{R132H}* (MGG18-IDH) (21) had no DLL3 expression by Western blot (Figure 5).

We then tested whether patient-derived, endogenous *IDH* mutant glioma tumorsphere lines could be killed with an agent that targets cell surface DLL3. We compared the effects of a DLL3-targeting ADC (SC16LD6.5, Rova-T) (24) and an IgG1 control ADC (IgGLD6.5) on the cell viability of *IDH* mutant and wildtype cells. In cells expressing DLL3, Rova-T is specifically internalized and trafficked to late endosomes and induces cytotoxicity (24). In cell vibility assays we found that the *IDH* mutant tumorsphere lines MGG119 and MGG152, both of which express high levels of DLL3, were sensitive to SC16LD6.5 and resistant to control ADC at picomolar concentrations (Figure 5). Cells without DLL3 expression were resistant to both ADCs. Therefore, our endogenous *IDH* mutant patient-derived glioma tumorspheres expressed high levels of DLL3 and were highly sensitive to Rova-T, whereas cells lacking DLL3 were resistant.

Discussion

Here, we found that the majority of *IDH* mutant gliomas homogeneously expressed the cell surface Notch ligand DLL3 whereas expression was patchy, low, or absent in *IDH* wildtype glioblastoma. Additionally, we found that patient-derived endogenous IDH mutant glioma tumorspheres, which overexpress DLL3, were potently and selectively sensitive to the anti-DLL3 ADC Rova-T in vitro. Therefore, we show that that DLL3 is a newly identified cell surface therapeutic target in *IDH* mutant glioma. Importantly, we found that DLL3 is rarely detected by IHC in non-tumor brain samples, which confirms a previous study that did not detect DLL3 protein in human brain tissue by sensitive enzyme-linked immunosorbent assay

assays (24) despite high levels of RNA being present in the brain (24, 40). These data indicate DLL3 is a tumor-associated antigen.

Our findings have potentially significant clinical impact. Rova-T is in clinical development for cancer (24, 28) and therefore our findings could be immediately translated to clinical trials in *IDH* mutant glioma. The limited protein expression in brain samples and the lack of central nervous system toxicity observed in early phase clinical trials of Rova-T (28) suggest targeting DLL3 in gliomas may be feasible. In addition, the cell surface localization of DLL3 and its homogeneous expression in *IDH* mutant glioma potentially opens the door for development of additional therapeutic strategies that exploit clonal cell surface antigens, such as adoptive cell transfer and other antibody-based targeting strategies.

Furthermore, the selectivity of DLL3 expression in gliomas may also provide insight into the developmental origins of glioma biological subgroups. In early brain development, *DLL3* expression is dynamic and occurs after neuroepithelial cells have ceased proliferating and before terminal differentiation into neurons. Therefore, DLL3-expressing cells may represent a population of post-mitotic neuroblasts on the verge of terminal neuronal differentiation (41, 42). It is intriguing to speculate that the progenitor cell of *IDH* mutant gliomas is a DLL3-expressing low proliferation rate neuroblast, and that *IDH* mutation and the subsequent epigenetic reprogramming induced by the mutation (8, 43–45) prevents terminal differentiation of neuroblasts into neurons. Evidence for the similarity of *IDH* mutant gliomas and neuroblasts exists in prior literature. In 2006, prior to the identification of cancer-associated *IDH1/2* mutations, Phillips et al. described high-grade glioma subtypes by expression profiling, including "proneural" and "mesenchymal" subtypes. High *DLL3* expression was the signature marker of proneural tumors (38), and later studies identified the major feature of the proneural gene expression subtype to be *IDH* mutation (39). Intriguingly, Phillips et al. noted that proneural and mesenchymal subtypes paralleled stages of neurogenesis in the adult forebrain, with proneural tumors resembling committed neuronal precursors such as low proliferation rate neuroblasts while mesenchymal tumors resembled neural stem cells and/or transit-amplifying cells (38).

Interestingly, the *DLL3* gene maps to 19q13, a region lost during whole-arm chromosome 19q loss of heterozygosity in the 1p/19q codeleted subset of *IDH* mutant gliomas. In our study, *IDH* mutant, 1p/19q codeleted gliomas universally expressed DLL3, with the majority showing highly homogeneous and intense expression. This indicates the hallmark genomic alteration of this glioma subtype and DLL3 expression may be functionally linked. Given the dynamic expression of DLL3 during neurogenesis, investigating the effect of *DLL3* loss of heterozygosity on DLL3 regulation may provide clues to the cell of origin and pathogenesis of 1p/19q codeleted tumors.

Our study would benefit from independent validation of DLL3 expression by IHC and *in vivo* validation of Rova-T in an *IDH* mutant glioma model. In addition, although DLL3 was expressed in the majority of tumor cells in *IDH* mutant gliomas in our validation set, median H scores were lower compared to the discovery set. We suspect the age of the NYU archival tumor blocks tested (33 of 36 tumor blocks were >10 years old and 28% were >20 years old), which could affect IHC efficiency due aging as well as the variation in the fixation,

processing and storage procedures over time, might account for some of the observed difference. Interestingly, we observed generally higher levels of expression in more recent tumors, although this difference was not statistically significant. In addition, it will be important to examine the level and pattern of DLL3 expression in a set of tumors recurrent after known adjuvant therapy as most of our paired tumors (10 paired tumors) received no treatment other than resection, and the adjuvant treatment was unknown for 3 others.

In conclusion, we have identified DLL3 as tumor associated antigen and a novel cell surface therapeuticl target in *IDH* mutant gliomas. Our finding has potential rapid clinical application and has implications for the development of novel therapeutic strategies that exploit cell surface tumor-specific antigens. Additionally, the tight association between DLL3 expression and *IDH* mutant glioma raises interesting questions regarding the cell of origin of *IDH* mutant glioma given the essential role of DLL3 in cell fate decisions during neurogenesis. Further investigation of the role of DLL3 in *IDH* mutant glioma development may provide additional clues to gliomagenesis as well as novel therapeutic targets.

Supplementary Material

Refer to Web version on PubMed Central for supplementary material.

Acknowledgments

References

1. Parsons DW, Jones S, Zhang X et al. An integrated genomic analysis of human glioblastoma multiforme. Science. 2008;321:1807–12. [PubMed: 18772396]

2. Yan H, Parsons DW, Jin G et al. IDH1 and IDH2 mutations in gliomas. N Engl J Med. 2009;360:765–73. [PubMed: 19228619]

3. Hartmann C, Meyer J, Balss J et al. Type and frequency of IDH1 and IDH2 mutations are related to astrocytic and oligodendroglial differentiation and age: a study of 1,010 diffuse gliomas. Acta Neuropathol. 2009;118:469–74. [PubMed: 19554337]

4. Lai A, Kharbanda S, Pope WB et al. Evidence for sequenced molecular evolution of IDH1 mutant glioblastoma from a distinct cell of origin. J Clin Oncol. 2011;29:4482–90. [PubMed: 22025148]

5. Patel SH, Poisson LM, Brat DJ et al. T2-FLAIR Mismatch, an Imaging Biomarker for IDH and 1p/19q Status in Lower-grade Gliomas: A TCGA/TCIA Project. Clin Cancer Res. 2017

6. Watanabe T, Nobusawa S, Kleihues P, Ohgaki H. IDH1 mutations are early events in the development of astrocytomas and oligodendrogliomas. Am J Pathol. 2009;174:1149–53. [PubMed: 19246647]

7. Dang L, White DW, Gross S et al. Cancer-associated IDH1 mutations produce 2-hydroxyglutarate. Nature. 2009;462:739–44. [PubMed: 19935646]

8. Turcan S, Rohle D, Goenka A et al. IDH1 mutation is sufficient to establish the glioma hypermethylator phenotype. Nature. 2012;483:479–83. [PubMed: 22343889]

9. Bettegowda C, Agrawal N, Jiao Y et al. Mutations in CIC and FUBP1 contribute to human oligodendroglioma. Science. 2011;333:1453–5. [PubMed: 21817013]

10. Jiao Y, Killela PJ, Reitman ZJ et al. Frequent ATRX, CIC, and FUBP1 mutations refine the classification of malignant gliomas. Oncotarget. 2012;3:709–22. [PubMed: 22869205]

11. Killela PJ, Reitman ZJ, Jiao Y et al. TERT promoter mutations occur frequently in gliomas and a subset of tumors derived from cells with low rates of self-renewal. Proc Natl Acad Sci U S A. 2013;110:6021–6. [PubMed: 23530248]

12. Killela PJ, Pirozzi CJ, Healy P et al. Mutations in IDH1, IDH2, and in the TERT promoter define clinically distinct subgroups of adult malignant gliomas. Oncotarget. 2014;5:1515–25. [PubMed: 24722048]

13. Ceccarelli M, Barthel FP, Malta TM et al. Molecular Profiling Reveals Biologically Discrete Subsets and Pathways of Progression in Diffuse Glioma. Cell. 2016;164:550–63. [PubMed: 26824661]

14. Shirahata M, Ono T, Stichel D et al. Novel, improved grading system(s) for IDH-mutant astrocytic gliomas. Acta Neuropathol. 2018

15. Johnson BE, Mazor T, Hong C et al. Mutational analysis reveals the origin and therapy-driven evolution of recurrent glioma. Science. 2014;343:189–93. [PubMed: 24336570]

16. Bai H, Harmanci AS, Erson-Omay EZ et al. Integrated genomic characterization of IDH1-mutant glioma malignant progression. Nat Genet. 2016;48:59–66. [PubMed: 26618343]

17. Wakimoto H, Tanaka S, Curry WT et al. Targetable signaling pathway mutations are associated with malignant phenotype in IDH-mutant gliomas. Clin Cancer Res. 2014;20:2898–909. [PubMed: 24714777]

18. Cairncross JG, Wang M, Jenkins RB et al. Benefit from procarbazine, lomustine, and vincristine in oligodendroglial tumors is associated with mutation of IDH. J Clin Oncol. 2014;32:783–90. [PubMed: 24516018]

19. Buckner JC, Shaw EG, Pugh SL et al. Radiation plus Procarbazine, CCNU, and Vincristine in Low-Grade Glioma. N Engl J Med. 2016;374:1344–55. [PubMed: 27050206]

20. Schumacher T, Bunse L, Pusch S et al. A vaccine targeting mutant IDH1 induces antitumour immunity. Nature. 2014

21. Tateishi K, Wakimoto H, Iafrate AJ et al. Extreme Vulnerability of IDH1 Mutant Cancers to NAD+ Depletion. Cancer Cell. 2015;28:773–84. [PubMed: 26678339]

22. Sulkowski PL, Corso CD, Robinson ND et al. 2-Hydroxyglutarate produced by neomorphic IDH mutations suppresses homologous recombination and induces PARP inhibitor sensitivity. Sci Transl Med. 2017;9

23. Karpel-Massler G, Ishida CT, Bianchetti E et al. Induction of synthetic lethality in IDH1-mutated gliomas through inhibition of Bcl-xL. Nat Commun. 2017;8:1067. [PubMed: 29057925]

24. Saunders LR, Bankovich AJ, Anderson WC et al. A DLL3-targeted antibody-drug conjugate eradicates high-grade pulmonary neuroendocrine tumor-initiating cells in vivo. Sci Transl Med. 2015;7:302ra136.

25. Chapman G, Sparrow DB, Kremmer E, Dunwoodie SL. Notch inhibition by the ligand DELTA-LIKE 3 defines the mechanism of abnormal vertebral segmentation in spondylocostal dysostosis. Hum Mol Genet. 2011;20:905–16. [PubMed: 21147753]

26. Serth K, Schuster-Gossler K, Kremmer E, Hansen B, Marohn-Köhn B, Gossler A. O-fucosylation of DLL3 is required for its function during somitogenesis. PLoS One. 2015;10:e0123776.

27. Geffers I, Serth K, Chapman G et al. Divergent functions and distinct localization of the Notch ligands DLL1 and DLL3 in vivo. J Cell Biol. 2007;178:465–76. [PubMed: 17664336]

28. Rudin CM, Pietanza MC, Bauer TM et al. Rovalpituzumab tesirine, a DLL3-targeted antibody-drug conjugate, in recurrent small-cell lung cancer: a first-in-human, first-in-class, open-label, phase 1 study. Lancet Oncol. 2017;18:42–51. [PubMed: 27932068]

29. Cerami E, Gao J, Dogrusoz U et al. The cBio cancer genomics portal: an open platform for exploring multidimensional cancer genomics data. Cancer Discov. 2012;2:401–4. [PubMed: 22588877]

30. Gao J, Aksoy BA, Dogrusoz U et al. Integrative analysis of complex cancer genomics and clinical profiles using the cBioPortal. Sci Signal. 2013;6:pl1.

31. Brennan CW, Verhaak RG, McKenna A et al. The somatic genomic landscape of glioblastoma. Cell. 2013;155:462–77. [PubMed: 24120142]

32. Cancer Genome Atlas Research N, Brat DJ, Verhaak RG et al. Comprehensive, Integrative Genomic Analysis of Diffuse Lower-Grade Gliomas. N Engl J Med. 2015;372:2481–98. [PubMed: 26061751]

33. Serrano J, Snuderl M. Whole Genome DNA Methylation Analysis of Human Glioblastoma Using Illumina BeadArrays. Methods Mol Biol. 2018;1741:31–51. [PubMed: 29392688]

34. Capper D, Jones DTW, Sill M et al. DNA methylation-based classification of central nervous system tumours. Nature. 2018;555:469–74. [PubMed: 29539639]

35. Bady P, Sciuscio D, Diserens AC et al. MGMT methylation analysis of glioblastoma on the Infinium methylation BeadChip identifies two distinct CpG regions associated with gene silencing and outcome, yielding a prediction model for comparisons across datasets, tumor grades, and CIMP-status. Acta Neuropathol. 2012;124:547–60. [PubMed: 22810491]

36. Kessler T, Sahm F, Sadik A et al. Molecular differences in IDH wildtype glioblastoma according to MGMT promoter methylation. Neuro Oncol. 2017

37. Hegi ME, Diserens AC, Gorlia T et al. MGMT gene silencing and benefit from temozolomide in glioblastoma. N Engl J Med. 2005;352:997–1003. [PubMed: 15758010]

38. Phillips HS, Kharbanda S, Chen R et al. Molecular subclasses of high-grade glioma predict prognosis, delineate a pattern of disease progression, and resemble stages in neurogenesis. Cancer Cell. 2006;9:157–73. [PubMed: 16530701]

39. Verhaak RG, Hoadley KA, Purdom E et al. Integrated genomic analysis identifies clinically relevant subtypes of glioblastoma characterized by abnormalities in PDGFRA, IDH1, EGFR, and NF1. Cancer Cell. 2010;17:98–110. [PubMed: 20129251]

40. Fagerberg L, Hallström BM, Oksvold P et al. Analysis of the human tissue-specific expression by genome-wide integration of transcriptomics and antibody-based proteomics. Mol Cell Proteomics. 2014;13:397–406. [PubMed: 24309898]

41. Dunwoodie SL, Henrique D, Harrison SM, Beddington RS. Mouse Dll3: a novel divergent Delta gene which may complement the function of other Delta homologues during early pattern formation in the mouse embryo. Development. 1997;124:3065–76. [PubMed: 9272948]

42. Ladi E, Nichols JT, Ge W et al. The divergent DSL ligand Dll3 does not activate Notch signaling but cell autonomously attenuates signaling induced by other DSL ligands. J Cell Biol. 2005;170:983–92. [PubMed: 16144902]

43. Lu C, Ward PS, Kapoor GS et al. IDH mutation impairs histone demethylation and results in a block to cell differentiation. Nature. 2012;483:474–8. [PubMed: 22343901]

44. Saha SK, Parachoniak CA, Ghanta KS et al. Mutant IDH inhibits HNF-4alpha to block hepatocyte differentiation and promote biliary cancer. Nature. 2014;513:110–4. [PubMed: 25043045]

45. Modrek AS, Golub D, Khan T et al. Low-Grade Astrocytoma Mutations in IDH1, P53, and ATRX Cooperate to Block Differentiation of Human Neural Stem Cells via Repression of SOX2. Cell Rep. 2017;21:1267–80. [PubMed: 29091765]

Statement of Translational Relevance

IDH mutant glioma is a clinically, radiographically, and biologically distinct subtype of malignant glioma that is molecularly divergent from *IDH* wildtype primary glioblastoma. Although *IDH* mutant gliomas are sensitive to radiation and chemotherapy, most tumors eventually recur and become fatal as no therapy is effective at recurrence. Here, we show that the Notch ligand DLL3 is intensely and homogeneously expressed in *IDH* mutant gliomas and high DLL3 expression is tightly associated with *IDH* mutant gliomas compared to other glioma subtypes. Furthermore, we show that an anti-DLL3 antibody drug conjugate is potently and selectively cytotoxic to patient-derived *IDH* mutant glioma tumorspheres. Our findings have potential for rapid clinical translation given the current clinical development of DLL3-targeting therapies. Additionally, the near ubiquitous and cell surface expression in tumors may enable the development of novel therapeutic strategies that exploit cell membrane tumor associated antigens.
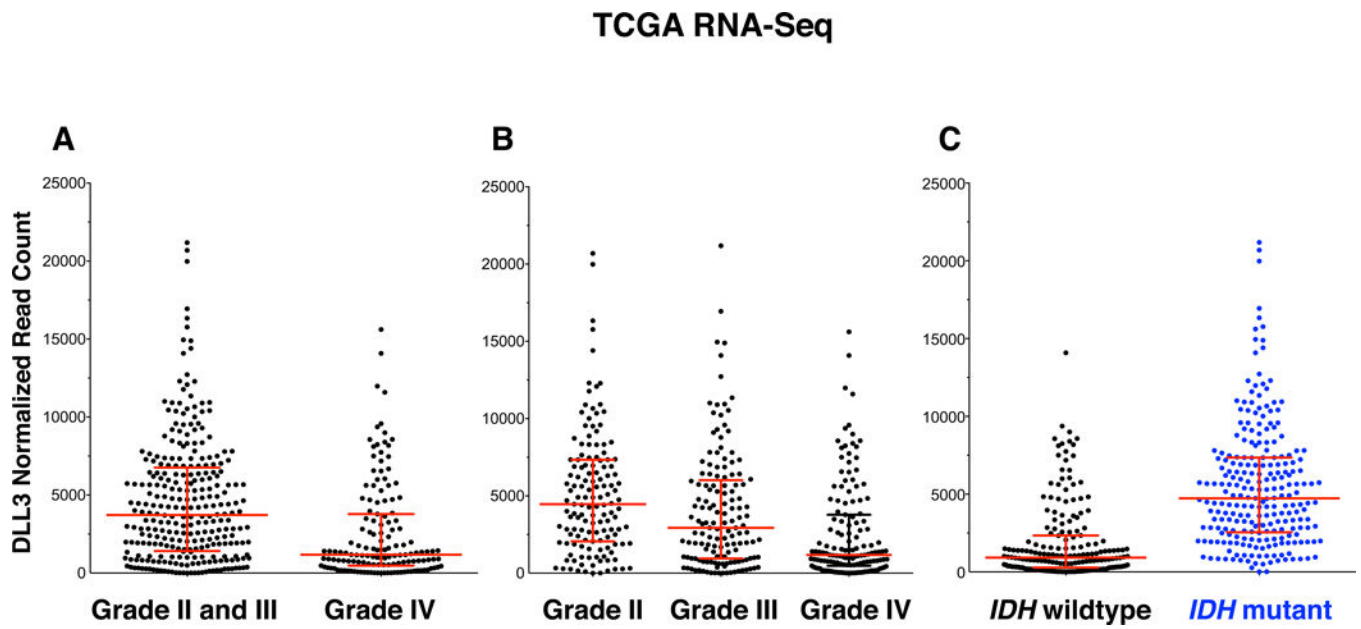
TCGA RNA-Seq

Figure 1. Elevated expression of DLL3 mRNA in *IDH* mutant glioma.
Shown are mapped reads to DLL3 transcripts as determined by whole transcriptome RNA-sequencing in TCGA tumor samples. (A) and (B) DLL3 mRNA reads by glioma grade. (C) DLL3 mRNA reads by IDH mutation status.
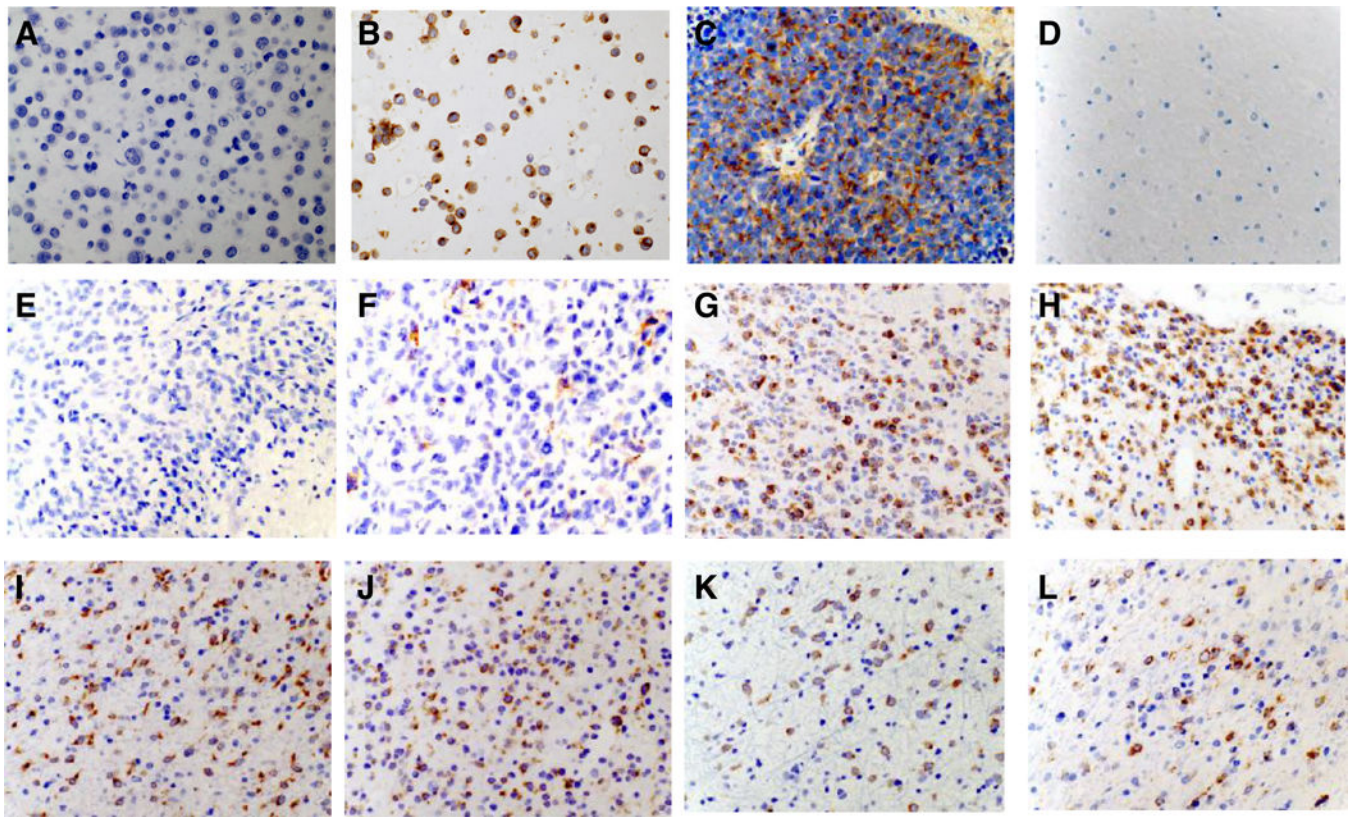
Figure 2. DLL3 expression in gliomas by immunohistochemistry.
Representative immunohistochemistry images using SC16.65, a monoclonal anti-DLL3 antibody. All images were acquired at 40X magnification. (A) Negative control cell line HEK-293T. (B) Positive control cell line HEK-293T.hDLL3. (C) Positive control patient-derived small cell lung cancer xenograft (ref 24). (D) Non-tumor brain sample. (E) *IDH* wildtype glioblastoma, Mesenchymal subtype. (F) *IDH* wildtype glioblastoma, RTKII subtype. (G) *IDH* mutant astrocytoma (non-codeleted) (H) *IDH* mutant oligodendroglioma, 1p/19q codeleted. (I-L) Examples of initial and paired recurrent tumors. (I) Initial *IDH* mutant astrocytoma (non-codeleted) and recurrent (J) tumor after initial treatment with resection only. (K) Initial *IDH* mutant astrocytoma (non-codeleted) and recurrent (L) tumor 17 years after resection followed by radiation treatment.
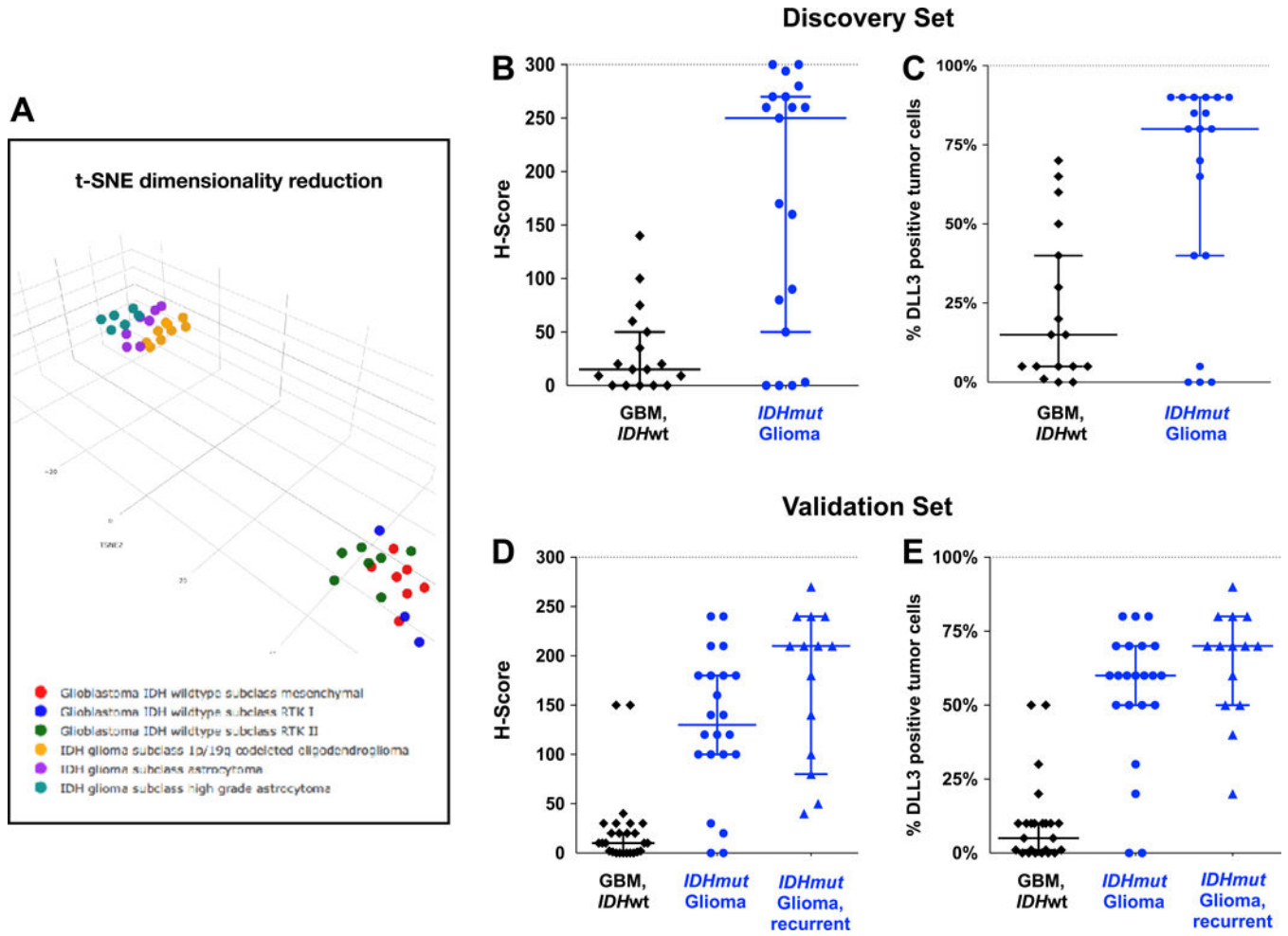
Figure 3. Elevated expression of DLL3 in *IDH* mutant gliomas by immunohistochemistry.
(A) Unsupervised clustering of discovery set samples using t-distributed stochastic neighbor embedding (t-SNE) dimensionality reduction. Individual samples are color-coded in the respective class color as described in the label. (B–C) DLL3 immunohistochemistry (IHC) scores of gliomas in the discovery set, distinguished by *IDH* mutation status. (B) IHC scored by Abbvie Stemcentrx. (C) IHC scored independently by NYU. Scoring was performed prior to determination of *IDH* mutation status. (C–D) DLL3 IHC scores of gliomas in the validation set, distinguished by *IDH* mutation status, and IDH mutant gliomas were further separated into initial and recurrent tumors. Bars represent median and 95% confidence intervals. Abbreviations: GBM, glioblastoma; *IDH*wt, *IDH* wildtype; *IDH*mut, *IDH* mutant.
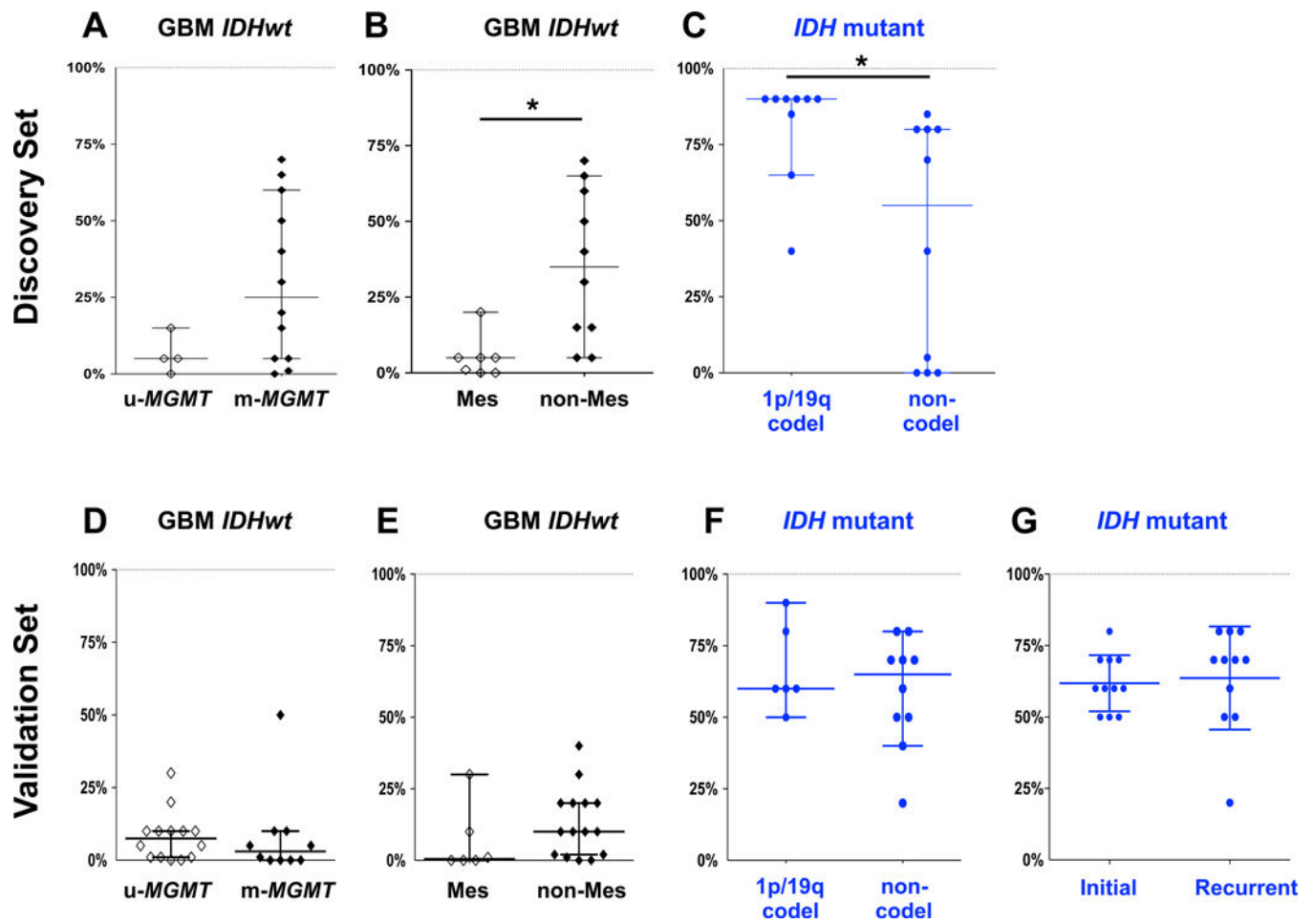
Figure 4. DLL3 expression by immunohistochemistry in gliomas molecular subtypes.
DLL3 IHC scores of glioma molecular subtypes determined by DNA methylation array classifier were compared. (A–C) Discovery set. (D–G) Validation set. Y axis represents the percentage of DLL3 positive tumor cells. Bars represent median and 95% confidence intervals. *, $P < 0.01$. Abbreviations: GBM, glioblastoma; *IDH*wt, *IDH* wildtype; u-*MGMT*, unmethylated *MGMT*; m-*MGMT*, methylated *MGMT*; Mes, Mesenchymal; codel, 1p/19q codeleted.
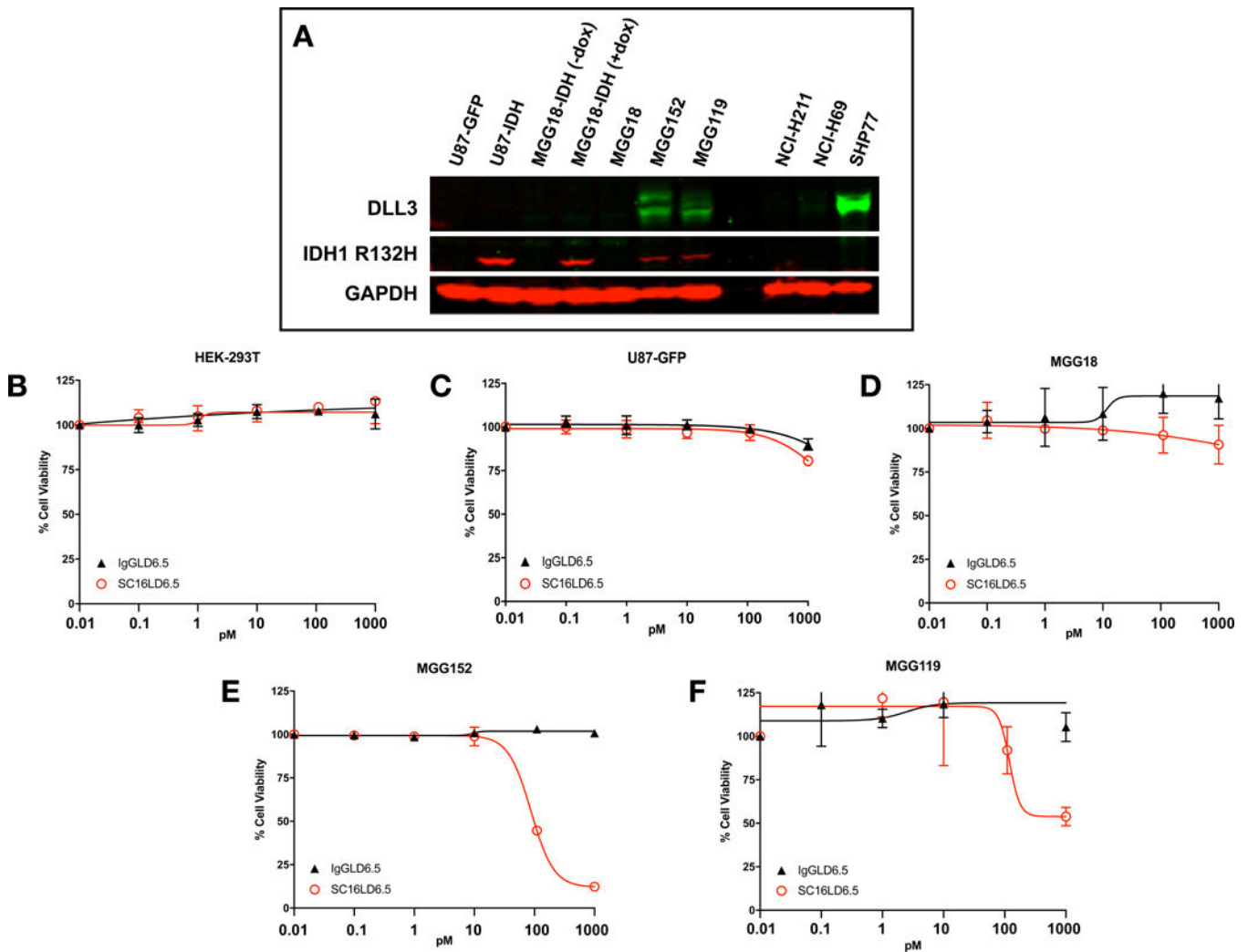
Figure 5. Patient-derived endogenous IDH mutant glioma tumorspheres overexpress DLL3 and are sensitive to an antibody drug conjugate targeting DLL3 (Rova-T).
(A) Western blot using antibodies against DLL3, the IDH1 R132H mutant enzyme, and actin (loading control). Lane labels: U87-GFP: an *IDH* wildtype glioma cell line (U87) engineered to overexpress GFP; U87-IDH: U87 constitutively overexpressing IDH1 R132H; MGG18-IDH (-dox): An *IDH* wildtype patient-derived glioblastoma tumorsphere line (MGG18) engineered with a doxycycline-inducible IDH1 R132H gene (MGG18-IDH), cultured without doxycycline; MGG18-IDH (+dox): MGG18-IDH cultured with doxycycline for 72 hours; MGG18: An *IDH* wildtype patient-derived glioblastoma tumorsphere line; MGG152: An patient-derived glioblastoma tumorsphere line with endogenous IDH1 R132H. MGG119: An patient-derived glioblastoma tumorsphere line with endogenous IDH1 R132H. NCI-H211: cell line known to lack DLL3 expression (negative control). NCI-H69: Cell line with low to medium DLL3 expression (control). SHP77: Cell line with high DLL3 expression (positive control). (B–E) Cells treated with a DLL3-targeting antibody-drug conjugate (ADC) SC16LD6.5 (Rova-T, red) or a non-targeting ADC (IgGLD6.5, black). (B) HEK-293T cells (no DLL3 expression) (ref 24). (C) U87-GFP (no DLL3 expression). (D) MGG18, an *IDH* wildtype patient-derived GBM

tumorsphere line with no to minimal DLL3 expression. (E) MGG152, an endogenous *IDH* mutant patient-derived GBM tumorsphere line with high DLL3 expression (F) MGG119, an endogenous *IDH* mutant patientderived GBM tumorsphere line with medium to high DLL3 expression.

Table 1.

DLL3 Immunohistochemistry Summary

	n	H-score median (95% CI)	P	DLL3+ cells median (95% CI)	P	DLL3+ tumor cells				
						0%	1–5%	6–49%	50–79%	80%
Discovery Set										
IDH wildtype GBM	17	15 (0–50)	**0.0007** (all 3 groups)	15% (5–40%)	**0.002** (all 3 groups)	2	6	5	4	0
IDH mutant glioma	19	250 (50–270)	**0.0014** (vs IDHwt GBM)	80 (40–90%)	**0.003** (vs IDHwt GBM)	3	1	2	2	11
Glioma variants	10	0 (0–50)		0.5% (0–70%)		5	2	1	1	1
Validation Set										
IDH wildtype GBM	26	10 (1–20)		5% (1–10%)		6	8	10	2	0
IDH mutant glioma	22	130 (100–180)	**0.0000043** (vs IDHwt GBM)	60% (50–70%)	**0.00000017** (vs IDHwt GBM)	2	0	2	15	3
Recurrent IDH mutant glioma	14	210 (80–240)	0.085 (vs non-rec IDHmut)	70% (50–80%)	0.16 (vs non-rec IDHmut)	0	0	2	8	4

DLL3 immunohistochemistry was performed at Abbvie Stemcentrix for the Discovery set and at NYU for the Validation set.

Immunostains were scored by two independent teams and prior to determination of the molecular status of the tumors. The Abbvie Stemcentrx team generated H-scores and the NYU team reported the percent of DLL positive (DLL3+) tumor cells.

Abbreviations: IDHwt, IDH wildtype; IDHmut, IDH mutant; non-rec, non-recurrent.